



## QUASIELASTIC NEUTRON SCATTERING STUDY OF LARGE AMPLITUDE MOTIONS IN MOLECULAR SYSTEMS

M. BÉE

*Laboratoire de Spectrométrie Physique, Université J. Fourier - Grenoble 1,  
B.P. 87 38402 Saint-Martin d'Hères Cedex, France*

### ABSTRACT

This lecture aims at giving some illustrations of the use of Incoherent Quasielastic Neutron Scattering in the investigation of motions of atoms or molecules in phases with dynamical disorder. The general incoherent scattering function is first recalled. Then the Elastic Incoherent Structure Factor is introduced. It is shown how its determination permits to deduce a particular dynamical model. Long-range translational diffusion is illustrated by some experiments carried out with liquids or with different chemical species intercalated in porous media. Examples of rotational motions are provided by solid phases where an orientational disorder of the molecules exists. The jump model is the most commonly used and yields simple scattering laws which can be easily handled. Highly disordered crystals require a description in terms of the isotropic rotational diffusion model. Many of the present studies are concerned with rather complicated systems. Considerable help is obtained either by using selectively deuterated samples or by carrying out measurements with semi-oriented samples.

### 1. Introduction

Incoherent Quasielastic Neutron Scattering (IQNS) is a technique which provides information about both the dynamical and the geometrical aspects of motions of molecules. The term "Incoherent" neutron scattering refers to a scattering process in which the neutron interacts with the same scatterer at two successive times. "Quasielastic" scattering is mainly interested in small energy-transfers, typically  $\pm 2$  meV ( $\pm 16$  cm<sup>-1</sup>) which originate from interactions of the neutrons with particles moving over time-scale c.a.  $10^{-10}$  –  $10^{-12}$  s. Such phenomena introduce a broadened component under the elastic line originating itself from the neutrons scattered without energy-change. An accurate investigation of the exact shape of this quasielastic component and a comparison of its relative amount with respect to the purely elastically scattered intensity yield the Elastic Incoherent Structure Factor (EISF), i.e. the long-time limit of the intermediate scattering function, which is directly related to the region of space accessible to a scatterer and contains precise information about the geometry of the motions. The characteristic times associated to the different motions are determined from the width of the broadened part and their temperature-dependence gives an idea of the potential barriers against the reorientations. A flourishing development of theoretical models has made the IQNS technique complementary to infrared or Raman light-spectroscopy, nuclear magnetic resonance, dielectric relaxation and X-rays.

## 2. Basic aspects of IQNS

The incoherent scattering function  $S(\vec{Q}, \omega)$ , where  $\vec{Q}$  is the momentum transfer vector and  $\hbar\omega$  the energy gain for the neutron is the time-Fourier transform

$$S(\vec{Q}, \omega) = \frac{1}{2\pi} \int_{-\infty}^{\infty} I(\vec{Q}, t) e^{-i\omega t} dt \quad (1)$$

of the intermediate scattering function  $I(\vec{Q}, t)$ . The latter is itself given, by the correlation function

$$I(\vec{Q}, t) = \left\langle e^{i\vec{Q} \cdot \vec{r}(t)} e^{-i\vec{Q} \cdot \vec{r}(0)} \right\rangle \quad (2)$$

where  $\vec{r}(t)$  and  $\vec{r}(0)$  are the positions vectors of the scatterer at time  $t$  and at time 0, respectively. Translational, rotational and vibrational motions change the position vector of the scattering nucleus. A common hypothesis generally assumes the dynamical independence of these motions so that  $I(\vec{Q}, t)$  is expressed as the product of the three contributions.

$$I(\vec{Q}, t) = I_{trans}(\vec{Q}, t) \cdot I_{rot}(\vec{Q}, t) \cdot I_{vib}(\vec{Q}, t) \quad (3)$$

Molecular vibrations occur on a time-scale much shorter than the diffusive processes and finally  $S(\vec{Q}, \omega)$  can be separated into two parts [1]

$$S(\vec{Q}, \omega) = e^{-\langle u^2 \rangle Q^2} \cdot \{ S_{quasi}(\vec{Q}, \omega) + S_{inel}(\vec{Q}, \omega) \} \quad (4)$$

The Debye-Waller factor  $e^{-\langle u^2 \rangle Q^2}$  takes care of all lattice and molecular vibrations. The inelastic term  $S_{inel}(\vec{Q}, \omega)$  is directly related to the frequency distribution of the vibrations and contributes little in the quasielastic region.  $S_{quasi}(\vec{Q}, \omega)$  is a quasielastic term which contains the effects due to translational and rotational motions. If any coupling is neglected,  $S_{quasi}(\vec{Q}, \omega)$  is simply the convolution product

$$S_{quasi}(\vec{Q}, \omega) = S_{trans}(\vec{Q}, \omega) \otimes S_{rot}(\vec{Q}, \omega) \quad (5)$$

of the scattering laws  $S_{trans}(\vec{Q}, \omega)$  and  $S_{rot}(\vec{Q}, \omega)$  for translational and rotational motions, respectively. Each intermediate scattering function  $I_{trans}(\vec{Q}, t)$  and  $I_{rot}(\vec{Q}, t)$  can be formally splitted into its constant limit at infinite time  $I(\vec{Q}, \infty)$  and its time-dependent part. Therefore both  $S_{trans}(\vec{Q}, \omega)$  and  $S_{rot}(\vec{Q}, \omega)$  can be written as:

$$S(\vec{Q}, \omega) = I(\vec{Q}, \infty) \delta(\omega) + S^{qe}(\vec{Q}, \omega) \quad (6)$$

where

$$S^{qe}(\vec{Q}, \omega) = \frac{1}{2\pi} \int_{-\infty}^{\infty} [I(\vec{Q}, t) - I(\vec{Q}, \infty)] e^{-i\omega t} dt \quad (7)$$

The scattering function appears composed of a purely elastic contribution superposed on a broadened component,  $S^{\text{qe}}(\vec{Q}, \omega)$ , the overall width of which is directly related to the characteristic times of the motions (Fig. 1).

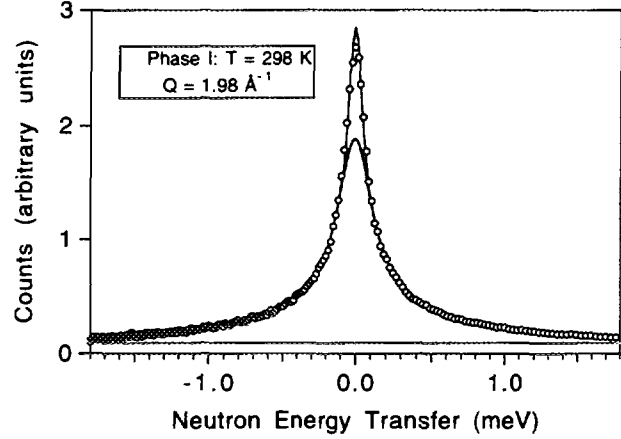


Fig. 1: Example of quasielastic spectrum obtained in the disordered phase of sulpholan. The separation between the purely elastic and the quasielastic part is indicated as obtained from the refinement of the theoretical scattering function.

At infinite time the system relaxes to the equilibrium distribution of the scatterer:

$$I(\vec{Q}, \infty) = \left\langle e^{i\vec{Q}\cdot\vec{r}(\infty)} e^{-i\vec{Q}\cdot\vec{r}(0)} \right\rangle = \left\langle e^{i\vec{Q}\cdot\vec{r}(0)} \right\rangle^2 \quad (8)$$

As defined by Eq. 8  $I(\vec{Q}, \infty)$  is a measure of the spatial equilibrium distribution of the scatterer. It vanishes in the case of long-range translational diffusion but any restriction in the volume of the space accessible to the scatterer yields a finite value of  $I(\vec{Q}, \infty)$ . More precisely, in the case of a scattering particle moving freely inside a volume  $V$ , the probability to find the scatterer in the unit volume around any given point  $\vec{r}(\infty)$  at infinite time is simply  $V^{-1} \rightarrow 0$  for sufficiently large volume  $V$ , so that  $I(\vec{Q}, \infty) = 0$ . Therefore a characteristic feature of the scattered intensity from a liquid or any material with dynamical translational disorder, like hydrogen in metals, superionic or protonic conductors, etc, is the absence of elastic peak (if  $Q \neq 0$ ). Conversely, the existence of an elastic component in the scattered intensity indicates the presence in the sample of a scatterer, the motion of which is essentially located in space (as in the case of rotational motions). It should be noted that the instrument resolution introduces a long-time limit in the determination of  $I(\vec{Q}, t)$  beyond which  $I(\vec{Q}, \infty)$  cannot be measured (the delta-function appears in the experimental spectra as a sharp peak with finite width).

By integrating the incoherent scattering law over the energy transfer  $\hbar\omega$  at constant  $\vec{Q}$  we get, from Eq. 1

$$\int_{-\infty}^{\infty} S(\vec{Q}, \omega) d\omega = \int_{-\infty}^{\infty} I(\vec{Q}, t) \delta(t) dt = I(\vec{Q}, 0) = 1 \quad (9)$$

$I(\vec{Q}, \infty)$  is the fraction of the total quasielastic intensity contained in the purely elastic peak. It is called the Elastic Incoherent Structure Factor (EISF). Providing that the separation between the sharp, purely elastic, component and the wider, quasielastic

contribution can be performed, the EISF is a measurable quantity evaluated for each modulus and direction of the momentum transfer,  $\vec{Q}$ , by the ratio

$$A(\vec{Q}) = \frac{I^{el}(\vec{Q})}{I^{el}(\vec{Q}) + I^{qe}(\vec{Q})} \quad (10)$$

where  $I^{el}(\vec{Q})$  and  $I^{qe}(\vec{Q})$  are the integrated intensities corresponding to the elastic and quasielastic part of the spectra.

### 3. Long-range translational diffusion

Neutron studies have stimulated several types of descriptions. The most simple is the continuous diffusion according to the Fick's law. It corresponds on the microscopic scale to the Brownian motion of particles and yields a lorentzian-shaped scattering function. The broadening varies as  $DQ^2$  and thus enables the determination of the diffusion constant  $D$ . A good example is provided by liquid argon. Hydrogen diffusion in solids rather occurs through a jump-diffusion mechanism: the Chudley-Elliott model [2] shows a departure from the  $DQ^2$  law. The Singwi-Sjölander model [3] takes into account successive oscillatory and diffusive states and was elaborated to interpret the mechanism of diffusion of molecules in water. These models were also used to describe the diffusion of various chemical species (methane, ethane, propane) adsorbed in the cavities of zeolites [4].

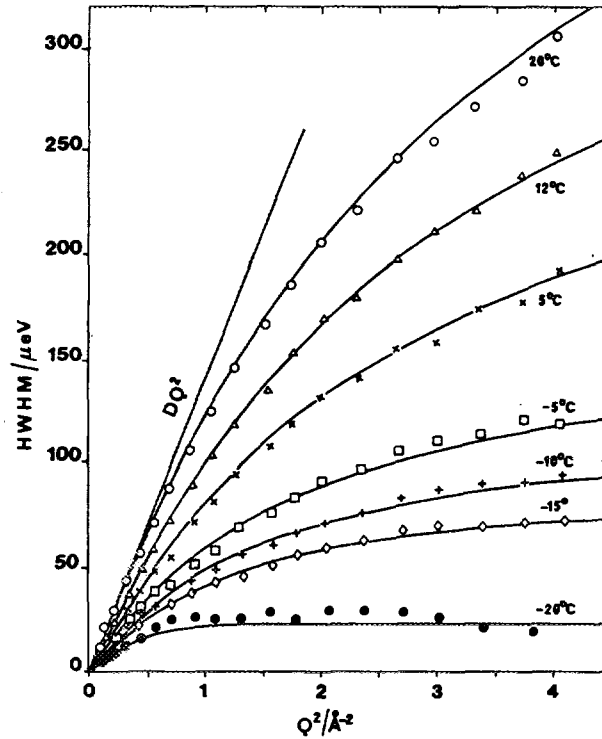


Fig. 2: Evolution of broadening of the spectra as a function of the momentum transfer for liquid water and comparison with the Singwi-Sjölander model. The deviation from the Fick's law is illustrated.

#### 4. Reorientations about a single axis

The one-proton incoherent reorientational scattering function corresponding to a jump-model among  $N$  equivalent positions equally spaced over a circle of radius  $r$  is well known [1, 5, 6]. A very simple case is provided by  $120^\circ$ -rotations. The scattering law involves a single quasielastic component and reads (for a powder sample):

$$S(Q, \omega) = A_0(Q)\delta(\omega) + A_1(Q)\frac{1}{\pi} \frac{\tau}{1 + \omega^2 \tau^2} \quad (11)$$

The expressions of the structure factors are

$$A_0(Q) = \frac{1}{3} [1 + 2j_0(Qr\sqrt{3})] \quad (12a)$$

$$A_1(Q) = \frac{2}{3} [1 - j_0(Qr\sqrt{3})] \quad (12b)$$

where  $j_0(Qr\sqrt{3})$  denotes the spherical Bessel function and  $r$  is the rotation radius.

An example of application of this model is provided by the rotation of methyl groups about their threefold axis, as observed in many polymers (polyacetaldehyde, polydimethylsiloxane, polypropylene, polymethylmethacrylate [7]) or biopolymers [8].

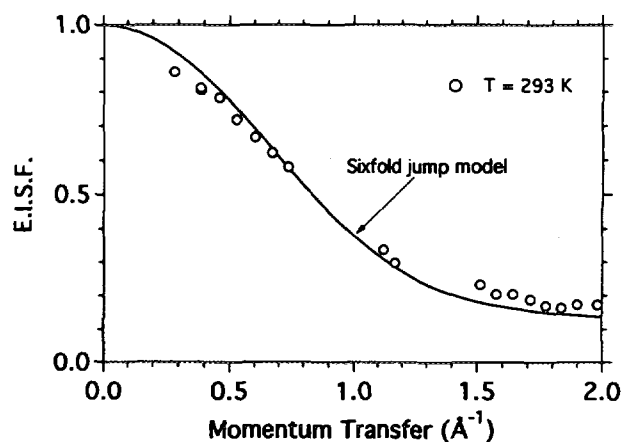


Fig. 3: Experimental values of the EISF in the disordered phase of sulpholan and comparison with the theoretical variation predicted by the jump model over six-sites.

Reorientations over a larger number of sites are observed with molecular compounds.  $C_5H_5$  rings of nickelocene undergo  $2\pi/5$  - jumps. In the disordered high-temperature phase of sulpholan (h.c.p.), the molecules reorient about their own twofold axis by  $60^\circ$  jumps (Fig. 3). A larger number of sites was found in the case of cyanoadamantane  $C_{10}H_{15}CN$ . The f.c.c. structure of the lattice is achieved by a stochastic distribution of the molecules along the lattice [100] axes. Because of the threefold symmetry of cyanoadamantane, the molecules jump among 12 sites around each lattice axis so that the fourfold symmetry of these directions is maintained.

## 5. Reorientations about several axes

Adamantane  $C_{10}H_{16}$  (tricyclo[3, 3, 1, 1<sup>3,7</sup>]decane is a cage-like molecule with tetrahedral symmetry. The cubic symmetry (Fm3m) of the room-temperature phase is achieved by a disorder of the molecules which can occupy two distinguishable orientations, related by  $90^\circ$ -rotations about the [100] axes of the f.c.c cell, the molecule and lattice threefold axes being coincident. Group theory leads to 5 characteristic times ( $\tau_1, \tau_2, \tau_3, \tau_4, \tau_5$ ), related to each of the irreducible representations ( $A_1, A_2, E, T_1, T_2$ ) of the  $O$  group. Their expressions involve the average times between two successive jumps about each lattice direction:  $90^\circ$  rotations about [100] axes ( $\tau_{C_4}$ ),  $180^\circ$  rotations about [110] axes ( $\tau_{C_2}$ ),  $120^\circ$  jumps about [111] axes ( $\tau_{C_3}$ ) and  $180^\circ$  jumps about [100] axes ( $\tau_{C_2}$ ).

$$\begin{aligned}
 \frac{1}{\tau_1} &= 0, & (A_1) \\
 \frac{1}{\tau_2} &= \frac{2}{\tau_{C_2}} + \frac{2}{\tau_{C_4}}, & (A_2) \\
 \frac{1}{\tau_3} &= \frac{1}{\tau_{C_2}} + \frac{3}{2\tau_{C_3}} + \frac{1}{\tau_{C_4}}, & (E) \\
 \frac{1}{\tau_4} &= \frac{1}{3\tau_{C_2}} + \frac{2}{3\tau_{C_2}} + \frac{1}{\tau_{C_3}} + \frac{4}{3\tau_{C_4}}, & (T_1) \\
 \frac{1}{\tau_5} &= \frac{4}{3\tau_{C_2}} + \frac{4}{3\tau_{C_2}} + \frac{1}{\tau_{C_3}} + \frac{4}{3\tau_{C_4}}, & (T_2)
 \end{aligned} \tag{13}$$

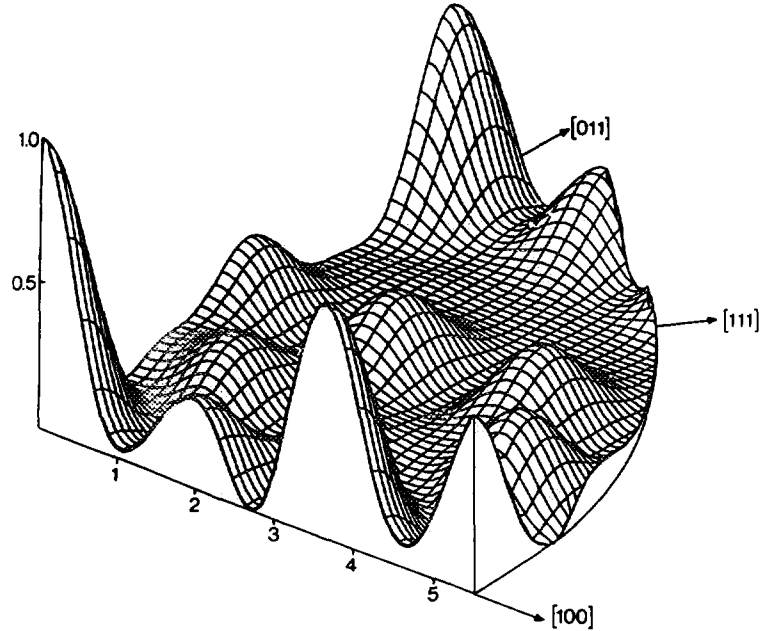


Fig. 4: Variation of the EISF corresponding to the model based on  $90^\circ$  jumps about [100] lattice directions as a function of the modulus and of the orientation of the momentum transfer vector in the plane of the reciprocal lattice containing the [100], [111] and [011] directions.

Three models can be envisaged depending on the occurrence of the different reorientations. When using a single crystal sample, the scattering law depends on the orientation of the scattering vector with respect to the specimen. Fig. 4 illustrates the variations of the EISF in the reciprocal lattice. In spite of the strong attenuation of the scattering arising from the large Debye-Waller factor which prevented the recording of accurate spectra at large momentum transfers ( $Q > 3.5 \text{ \AA}^{-1}$ ), experimental data could be analysed in terms of their purely elastic and quasielastic parts. The distinction could be made in favour of the  $90^\circ$ -jump model [9].

## 6. Reorientations about molecular and crystalline axes:

Group theory permits to calculate the scattering function when motions about both fixed (crystal) and mobile (molecular) axes are involved. Bicyclo-octane (BCO) and triethylenediamine (TEDA) are globular molecules, with the same symmetry. They show a phase transition from an hexagonal ordered phase to a high-temperature, f.c.c. plastic phase in which they reorient themselves between eight, equally weighted orientations with coincident threefold molecular and crystal axes. Around each  $[111]$  direction, there are two orientations separated by a  $60^\circ$ -rotation. The evolution of the characteristic times associated to each motion versus temperature suggests a stronger steric hindrance in TEDA than in BCO, in accordance with the lattice parameters at  $T = 300 \text{ K}$  ( $a = 8.86 \text{ \AA}$  and  $9.10 \text{ \AA}$  for TEDA and BCO respectively). The dominant role of the interatomic potential between nitrogen atom and other atoms was also evidenced [10].

Following the original study of adamantane, adamantanone  $\text{C}_{10}\text{H}_{14}\text{O}$  and several adamantane halides  $\text{C}_{10}\text{H}_{15}\text{X}$  ( $\text{X} = \text{F}, \text{Cl}, \text{Br}$ ) were extensively investigated in their plastic phase. According to the nature of the substituting atom on the adamantyl cage, the departure from globular symmetry is more or less important. The effects of steric hindrance were shown and all the experimental data could be interpreted in terms of jump-models based upon two types of reorientations.

## 7. Isotropic Rotational Diffusion (IRD)

Norbornane (NBA) exhibits at  $T = 306 \text{ K}$  a transition between an h.c.p. and a f.c.c. plastic phase. The IRD model was found well-adapted to describe the motions in both phases. In agreement with NMR, no discontinuity was observed for the rotational diffusion constant at the h.c.p.-f.c.c. phase transition:  $D_R = 2.03 \times 10^{12} \exp(-\Delta H/RT) \text{ s}^{-1}$  with the activation energy:  $\Delta H = 6.14 \text{ kJmol}^{-1}$ , in agreement with NMR [11]. At lower temperature, the EISF markedly deviates from the IRD model, but does not reduce into a uniaxial rotation. That was explained by the formation of ordered domains of close-packed molecules, the other remaining free to rotate. Similar effects are observed with hexamethylethane.

Norbornadiene (NBE) differs from NBA only by the presence of two double bonds. The liquid crystallises at  $254 \text{ K}$  either in a stable h.c.p. ( $a = 5.89 \text{ \AA}$ ,  $c = 9.51 \text{ \AA}$ ) or in a metastable f.c.c. structure ( $a = 8.80 \text{ \AA}$ ), depending on the conditions of cooling. The EISF is identical in both phases but the motions appear much less isotropic, even at the highest temperature, as compared with observed with NBA. In particular, no IRD is observed, because the EISF does not decrease to zero. A correct description requires a combination

of uniaxial reorientations with a simultaneous displacement of the centre of mass of c.a.  $0.6 \text{ \AA}$  [12]. The characteristic time of the motion follows an Arrhenius law:  $\tau = 2.5 \times 10^{12} \exp(\Delta H/RT) \text{ s}$  with the activation energy:  $\Delta H = 4.62 \text{ kJ.mol}^{-1}$ . In the liquid phase of NBE, a long-range displacement of the centre of mass of the molecules is responsible for an additional broadening of the spectra which can be described by the Chudley-Elliott model.

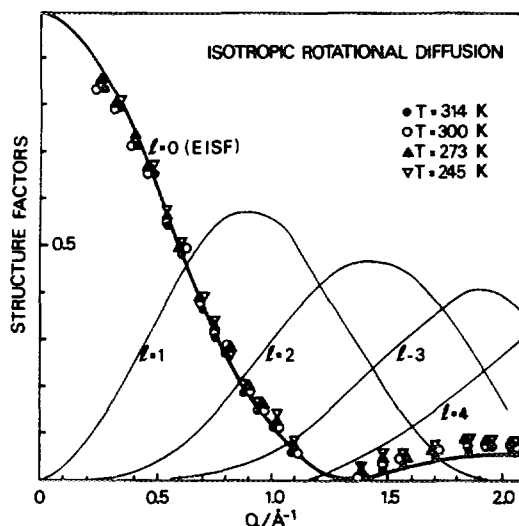


Fig. 5: Experimental values of the EISF in the disordered phase of norbornane and comparison with the theoretical variation predicted by the isotropic rotational diffusion model.

## 8. Columnar liquid-crystal phases.

Binuclear copper(II) complexes of fatty acids exhibit a phase transition from a lamellar crystalline lattice to a liquid crystalline mesophase. The latter structure is characterized by a two-dimensional hexagonal lattice where binuclear units are stacked and surrounded by alkyl chains pointing away from the Cu-Cu axis.

Dicopper complexes with various chain-lengths were compared by IQNS. From the EISF analysis large-amplitude motions were evidenced in the columnar and crystalline phases. Their amplitude continuously increases when increasing the length of the chain, and, together with the characteristic times they are temperature-dependent in all phases. It also appears that compounds with eight external chains are more disordered in their crystalline phase and less disordered in their columnar phase, with a more continuous change in the EISF at the transition.

An analysis with selectively deuterated dicopper palmitate samples revealed a different dynamics of the hydrogen atoms depending whether they are bound to carbons close to the core or far from it. Finally a similar behaviour of the part of the chain close to the core of the molecule, irrespective to the chain length, was evidenced.

Further investigations [13] were carried out with dicopper tetralaurate using spectrometers with a higher energy resolution available from the backscattering technique. The samples were pseudo-oriented fibres with the axes of the binuclear-core columns roughly parallel to the direction of the fibre. At the particular value of the scattering angle  $2\theta = 90^\circ$ , the momentum transfer vector was made successively parallel

and then perpendicular to the direction of the columns. Thus motions of the alkyl chains along the direction of the columns or about the column axes could be investigated separately. The difference observed between the spectra obtained for both geometries evidenced an anisotropic slow motion of the chains of the molecules around the axes of the columns.

## 9. Organic inclusion compounds.

$C_9H_{16}NO_2$ , (tano), forms stable crystalline inclusion compounds with linear alkanes. The guest molecules are enclosed end-to-end into parallel channels, 18 Å apart, with a diameter of 5 Å. There is a dynamical disorder of the alkyl chains inside the channels and also of the tano molecules, between their two chiral forms.

Earlier IQNS studies [14] dealt with tano/heptane and tano/octane and used selectively deuterated samples. Motions of the molecules of the matrix were evidenced, on two different time-scales. The faster motion was associated to  $CH_3$  rotations (correlation time  $\tau_{meth} = 1.9 \times 10^{-11}$  s at  $T = 290$  K, activation energy  $\Delta H = 12$  kJ.mol<sup>-1</sup>). The slower was attributed to the inversion of the tano cycle ( $\tau_{inv} = 3.9 \times 10^{-11}$  s at  $T = 320$  K). A further experiment on tano/hexadecane yielded a value of  $\tau_{inv}$ :  $9.8 \times 10^{-11}$  s at  $T = 320$  K. This was interpreted as a direct influence of the chain length on the cycle inversion, tano molecules near the ends of the guest chains being more disordered than molecules along the chains. The study of tano/bromohexadecane (tano/BrC<sub>16</sub>) and tano/bromodecane (tano/BrC<sub>10</sub>) confirms this result: a fraction of the methyl groups appears fixed. Their number increases with the length of the guest chain. Values of  $\tau_{meth}$  are slightly smaller than found in the earlier IQNS studies of tano/heptane and tano/octane where all the  $CH_3$  groups were considered as dynamically equivalent. Anyway, the activation energies for the methyl jumps ( $\Delta H = 12.6$  kJ.mol<sup>-1</sup> for tano/BrC<sub>16</sub> and  $\Delta H = 13.9$  kJ.mol<sup>-1</sup> for tano/BrC<sub>10</sub>) are consistent with the earlier value. The inversion of the tano cycle was recently observed by a high-resolution backscattering technique.

These studies concluded to 120°-jumps of the chains around the channel axis, and to faster local motions of the hydrogens involving displacements both parallel and perpendicular to the channel axis, due to local chain torsions. This latter motion was found related to the 120°-jumps of the alkyl and it was suggested that it could result from gauche or kink defects of the chains, induced by the flipping of the tano molecule between its chiral forms. Recent experiments on crystalline needles oriented along the channels evidenced the anisotropy of these displacements which occur rather around the channel axis than along it.

## 10. Conclusion

We tried, through a restricted series of examples, to give some idea of the information which can be obtained from IQNS. Considerable help in the choice of a model is obtained from the determination of the EISF, which shows the importance of the molecule delocalization. Although it is based on some hypotheses which are strictly not valid the jump model is the most commonly used and it is often able to give an adequate description of the motions. True IRD is rarely encountered, except in some cases of highly disordered crystals. Many of the present studies are concerned with rather

complicated systems. The final part of this lecture shows how considerable help is obtained either by using selectively deuterated samples or by carrying out measurements with semi-oriented samples. Thus in the case of columnar liquid crystals, the flexibility of the chains and the relative motions of their parts were investigated. In the case of inclusion compounds, the dynamics of the host matrix and of the guest alkyl chains were analysed separately.

## REFERENCES

1. M. Bée, *Quasielastic Neutron Scattering: Principles and Applications in Solid State Chemistry, Biology and Materials Science* (Adam Hilger, Bristol, 1988)
2. G. T. Chudley and R. J. Elliott, *Proc. Phys. Soc.* **77** (1961) 353
3. K. S. Singwi and A. Sjölander, *Phys. Rev.* **119** (1960) 863
4. H. Jobic, M. Bée and G. J. Kearley, *Zeolites* **12** (1992) 146
5. Dianoux, A.J., Volino, F. and Hervet, H., 1975, *Mol. Phys.* **30**, 1181
6. Hervet, H., Volino, F., Dianoux, A.J. and Lechner, R.E., 1974, *J. Phys. Lett.* **35**, L151
7. G. Allen, C. J. Wright and J. S. Higgins *Polymer* **15** (1975) 319
8. H. D. Middendorf and J. T. Randall, in *Structure and Motion: Membranes, Nucleic Acids and Proteins* ed. E. Clementi, G. Corongiu, M. H. Sarma and R.H. Sarma (Adenine, New-York, 1985)
9. M. Bée, J.P. Amoureux and R. E. Lechner, *Mol. Phys.* **39** (1980) 945
10. J. P. Amoureux, M. Bée and J.L. Sauvajol, *Mol. Phys.* **45** (1982) 709
11. M. Bée, H. Jobic and C. Caucheteux, *J. Chim. Phys.* **83** (1986) 10
12. M. Bée, J. Elkhamkhami and H. Jobic, *J. Phys.. Condensed Matter* **2** (1990) 1945
13. M. Bée, A.M. Giroud-Godquin, P. Maldivi, J.C. Marchon and J. Williams, *Mol. Phys.* **81** (1994) 57
14. M. Bée, A. Renault, J. Lajzėrowicz-Bonneteau and M. Le Bars-Combe, *J. Chem. Phys.* **97** 10 (1992) 7730